Molecular Vision 2006; 12:1674-86 <http://www.molvis.org/molvis/v12/a191/>
Received 31 August 2006 | Accepted 17 December 2006 | Published 24 December 2006

Immunocytochemical evidence that rod-connected horizontal cell axon terminals remodel in response to experimental retinal detachment in the cat

Kenneth A. Linberg,[1] Geoffrey P. Lewis,[1] Brian Matsumoto,[1,2] Steven K. Fisher[1,2]

[1]Neuroscience Research Institute, [2]Department of Molecular, Cellular and Developmental Biology, University of California, Santa Barbara, CA

Purpose: Cats have two types of horizontal cell (HC); one is axon-bearing (B-type), the other is axonless (A-type) [1,2]. We have previously described neurite sprouting from HCs in response to experimental retinal detachment [3]. Here we sought to determine whether one or both types elaborate these outgrowths.

Methods: Sections as well as wholemounts of retinas detached for 3, 7 and 28 days together with control retinas were double or triple labeled with antibodies to the calcium binding proteins calretinin and calbindin, to the synaptic vesicle-associated membrane protein 2 (VAMP2), and to the 70 and 200 kDa subunits of the neurofilament protein. Digital immunofluorescence images were collected by both confocal and two-photon microscopy.

Results: In control retina, both HC types label with antibodies to calretinin and calbindin D, but only the A-type also intensely labels with the neurofilament protein antibody. After 3, 7 and 28 days of detachment, these staining patterns persist, but there is a moderate upregulation of neurofilament protein in the B-type cell. In the detached retina, HC processes sprout neurites that appear most commonly as a loose array of fine beaded processes rising from the outer plexiform layer (OPL) into the outer nuclear layer (ONL), or, especially at 28 days, as stout unbranching processes that often cross the ONL en route to the subretinal space where some expand and arborize. Both types are strongly calretinin-positive while being somewhat less positive for antibodies to calbindin D and neurofilament protein. Moreover, they all arise from similarly labeled processes in the distal-most domain of the OPL where the narrowly stratified field of axon terminal boutons of the B-type HC normally innervates rod spherules, two to three thousand per cell [4]. Our data indicate that the HC sprouts apparently arise specifically from the axon terminal of the B-type cell since outgrowths were never seen arising from either type of HC perikaryon or from processes identifiable as A-type dendrites.

Conclusions: The data described here point to the specific remodeling of the rod-connected axon terminals of the B-type cell through neurite outgrowth. Rods respond to detachment by withdrawing synaptic terminals from the OPL while cones do not [5]. Those HC outgrowths that terminate within the ONL appear to retain their connection with the retracted terminals. Others apparently have lost their presynaptic targets and cross the ONL in association with hypertrophied Müller cell processes.

We have previously shown that experimental retinal detachment in a number of mammalian species induces morphological changes in photoreceptors [6], non-neuronal cells including Müller cells [5,7], and in other retinal neurons including horizontal, bipolar [3], and ganglion cells [8]. Photoreceptor changes include the loss of rod and cone outer segments as well as the retraction of many rod terminals from the outer plexiform layer (OPL) [3,7]. Changes in the horizontal cells (HCs) include the sprouting of neurites. While a few of these neurites extend into the inner nuclear layer (INL), most grow distally into the outer nuclear layer (ONL) [5]. Here we describe two types of such HC neurites: relatively thick processes that cross the ONL either singly or in loose arrays, or shorter, beaded processes that terminate within the ONL. The former traverse the ONL en route to the retinal surface often in association with hypertrophied Müller cells [5,8-10].

Correspondence to: Dr. Steven Fisher, University of California, Neuroscience Research Institute, University of California Santa Barbara, CA 93106; Phone: (805) 893-3637; FAX: 805 893-2005; email: fisher@lifesci.ucsb.edu

Cat retina has been shown to have two types of HC [1,2,11]. Figure 1, reproduced from Fisher and Boycott [1], depicts a Golgi-impregnated example of each type. The “A-type” axonless cell (HA) has long, stout tapering dendrites tipped by clusters of dendritic boutons. The axon-bearing “B-type” (HB) has short and somewhat finer radial dendrites on its somal end, and a large, multibranched axon terminal system on the other (HBat) decorated with thousands of terminal boutons. A thin, half-micron diameter non-branching axon connects the two parts of this cell. The camera lucida drawings mask the fact that various parts of these planar cells are narrowly but characteristically stratified: the thick axon terminal trunks as well as the dendritic trunks of both HC types lie at the inner edge of the OPL while the innervating dendritic and axonal telodendritic boutons lie at the outer edge of this layer. Fine dendritic branches that rise vertically through the OPL connect these trunks and terminals [12].

Kolb et al. [12] showed by Golgi EM that the dendrites of both types exclusively synapse with cones, while the axon terminal of the B-type synapses with rods only. The A-type

cell has a flattened perikaryon (see Figure 2A,B and Figure 3B, Figure 6A) while that of the B-type is rounded and protrudes further down into the INL (see Figure 2A,B and Figure 3B). She noted that the axon terminal boutons innervating the rod spherules lie at a level more distal than the dendrites innervating the cones. This correlates with the fact that rod spherules are stacked in many rows while cone pedicles tend to lie in one row along the distal border of the OPL. Unlike these examples of isolated Golgi-impregnated cells, dendrites of both types as well as the complex axon terminal systems all intertwine and each also tiles the retina as shown by Wässle et al. [13].

Immunostaining in general does not produce images of isolated cells so the problem we faced is how to visually dissect the tangle of labeled processes in the OPL in order to identify the origins of the outgrowths observed after detachment.

Portions of this study have been presented elsewhere in abstract form [14].

METHODS

Experimental retinal detachments were made in adult cat eyes as previously described [15]. The experimental use of the animals was conducted in compliance with both the guidelines of the UCSB IUCAC and the ARVO Statement for the Use of Animals in Ophthalmic and Vision Research.

Immunocytochemistry and confocal microscopy: The samples consisted of 100 μm thick vibratome sections as well as pieces of wholemounted cat retina from control retina as well as retinas detached for 3, 7, and 28 days. Tissue was fixed and processed as described elsewhere [3,16,17]. During these procedures, sections of agarose-embedded retina and pieces from wholemounts were labeled using the same protocol.

In order to immunocytochemically characterize the labeling signatures of the two types of HC as well as reveal their relationship to neighboring cells, we double or tripled labeled this tissue with various combinations of primary antibodies. We used antibodies to the 70 and 200 kDa subunits of the neurofilament protein (biotinylated; 1:100, Biomeda, Foster City, CA) specifically because the A-type HC in cat had been shown to be rich in these structures when examined by electron microscopy [1]. We chose antibodies to calbindin D (mouse monoclonal; 1:1000, Sigma, St. Louis, MO) and calretinin (rabbit polyclonal; 1:500, Chemicon, Temecula, CA) since both are known to label both types of cat horizontal cell [18-20]. An antibody to the synaptic protein VAMP2 (synaptobrevin; mouse monoclonal; 1:500, Synaptic Systems GmbH, Göttingen, Germany) was also used to visualize photoreceptor synaptic terminals. These primary antibodies were visualized using secondary antibodies conjugated with various fluorochromes: calretinin invariably with donkey, α-rabbit immunoglobulin G conjugated to the fluorochrome Cy3 (1:200; Jackson ImmunoResearch Laboratories, West Grove, PA); calbindin D with donkey, α-mouse immunoglobulin G conjugated to the fluorochrome Cy5 (1:200; Jackson ImmunoResearch Laboratories, West Grove, PA); synaptobrevin (vamp) with donkey, α-mouse immunoglobulin G conjugated to the fluorochrome Cy2 (1:200; Jackson ImmunoResearch Laboratories, West Grove, PA); and biotinylated neurofilament with streptavidin conjugated with either Cy2 or Cy5 (1:100, Jackson ImmunoResearch Laboratories, West Grove, PA). In order to avoid cross-reactivity, when we triple-labeled the tissue with antibodies to neurofilament in conjunction with calretinin and either VAMP2 or calbindin D, we labeled the tissue with the latter probes and their secondary antibodies prior to probing with the biotinylated

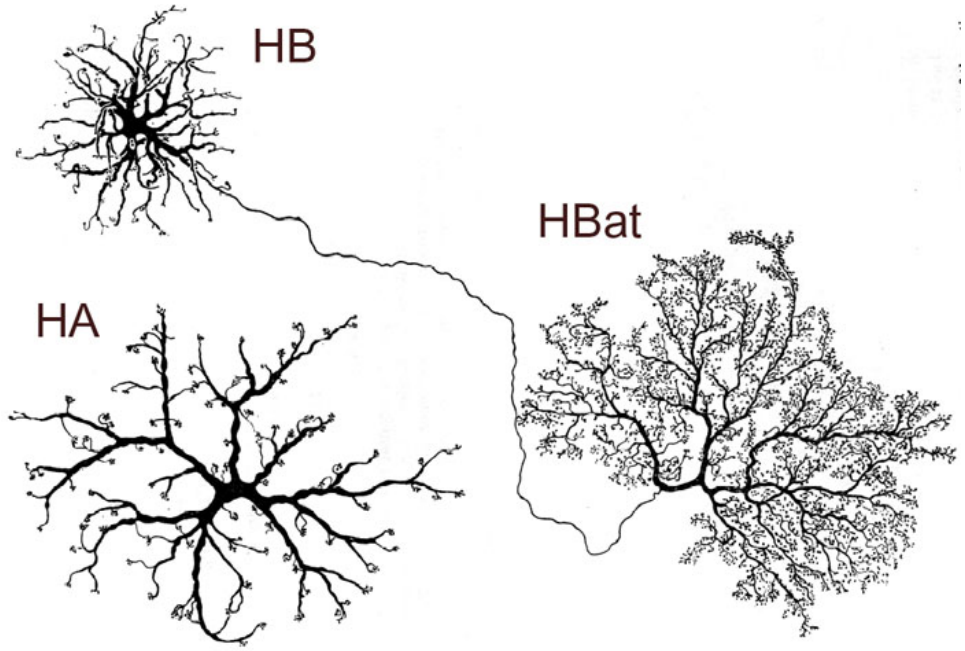

Figure 1. The two types of horizontal cell in Golgi-impregnated cat retina. Camera lucida drawings from Fisher and Boycott [1] of the two types of horizontal cell in Golgi-impregnated cat retina [2]. The dendrites of both the axonless A-type (HA) and the axon-bearing B-type (HB) contact cones only while the axon terminal system of the B-type (HBat) innervates rods exclusively [12]. Although these structures appear planar, they are not. The large dendritic and axon telodendrial trunks lie at the inner border of the outer plexiform layer (OPL) while the dendrites innervating both types of photoreceptor ramify at its outer border.

neurofilament protein antibody followed by its streptavidin-conjugated fluorochrome.

Image collection: Most images were collected using either a BioRad 500 or an Olympus Fluoview 500 confocal microscope. Using ImagePro Plus software (Media Cybernetics, San Diego, CA), a number of HC outgrowths from both the wholemounts and radial sections of detached retina were reconstructed from z series images taken at intervals of from 0.3 to 1 μm in depth. Some pieces of wholemounted retina were also examined with a Zeiss LSM 510 two-photon laser scanning microscope. In this case, the tissue protocol was altered such that the antibody to calretinin was conjugated with donkey-anti-rabbit aminomethylcoumarin (AMCA; Jackson ImmunoResearch Laboratories, West Grove, PA).

In collecting the images, especially when using multiple probes, the intensity was set for each channel and kept constant during each viewing session in order that the relative contribution of each probe could be assessed.

Image processing: The images in Figure 9 to Figure 14 were contrast enhanced with Adobe Photoshop CS to reveal structural details. In some cases this involved a reversal of contrast (Figure 9 through Figure 12). Rotated views of reconstructed image stacks were created using ImagePro Plus or Zeiss proprietary software and saved as movie files (Figure 11 through Figure 14). Movies were constructed from z series stacks containing the single image planes shown in Figure 11 through Figure 14.

RESULTS

Calretinin expression in normal cat retina: Figure 2A,B demonstrate the cell populations expressing calretinin immunoreactivity in normal cat retina: cell types similar to those described by Goebel and Pourcho [19]. Both types of HC label strongly with this antibody, the B-type cell more intensely than the flatter and more distally lying A-type cell (Figure 2A,B). Labeling intensity varies among amacrine cell types ("A" in Figure 2A), several ganglion cells types ("G" in Figure 2B), and calretinin-positive processes in the nerve fiber bundles (arrows in Figure 2A,B). AII amacrine cells (* in Figure 2A) show an intermediate labeling intensity in cat, unlike their more robustly labeled counterparts in rabbit [21,22] and monkey [23,24].

Double and triple immunofluorescent labeling: When the normal cat retina is triple labeled with antibodies to calretinin, calbindin D and neurofilament, the A-type HC and its processes are readily differentiated from the B-type cell (Figure 3A,B, Figure 4). The labeling of calretinin was assigned to the red channel, calbindin D to the blue channel, and neurofilament to the green channel. Since the A-type cells are labeled by all three probes they appear pinkish to bluish-white, while the axon bearing B-type cells, with almost undetectable α-neurofilament labeling and with a lower affinity for α-calbindin D [18], remain red. Note that the cell bodies of both types as well as the thicker dendritic trunks from each lie in the distal INL. Processes in the outer OPL are largely red although bluish to pink A-type dendrites are also seen (Figure 3A,B). As is evident here in control retina, there are no HC processes extending beyond the OPL into the ONL. However, HC outgrowths are indeed already present in retina detached for as little as three days (data not shown) [3]; such processes are even larger and more numerous after detachments of longer duration (Figure 5, Figure 6B through Figure 10).

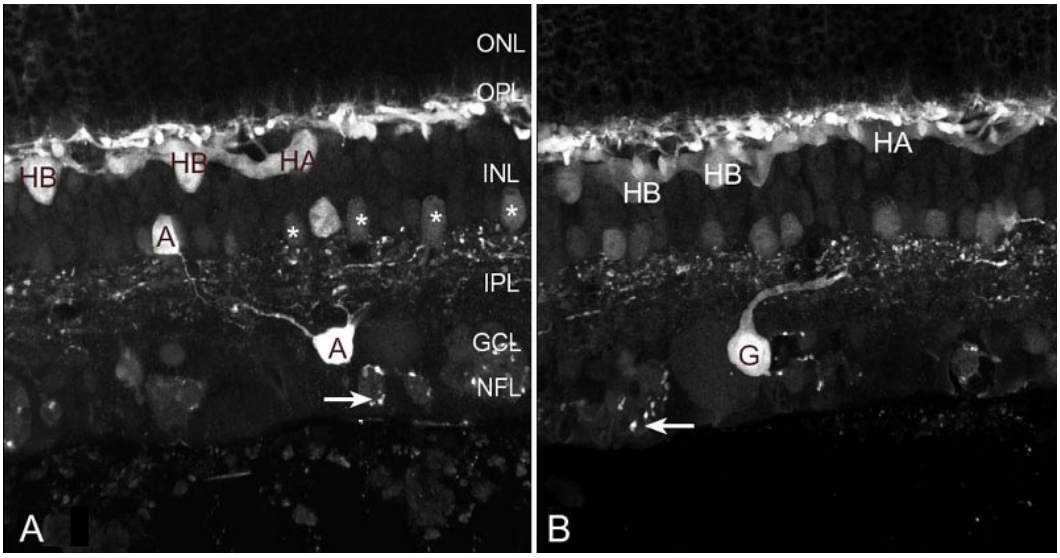

Figure 2. Confocal micrographs of the immunofluorescent labeling patterns of anti-calretinin in normal cat retina. Confocal micrographs of the immunofluorescent labeling patterns of anti-calretinin in normal cat retina. **A**: While the antibody to calretinin labels both types of HC (HA, HB), the B-type cell is labeled more intensely. Certain amacrine cell types (A) label brightly on both sides of the inner plexiform layer (IPL); others, notably the AII amacrine cells (*) label less robustly. A subpopulation of fibers in the nerve fiber bundles labels strongly with this antibody (arrows). **B**: In addition, a ganglion cell (G) is anti-calretinin-positive and sends its primary dendritic trunk into the mid-IPL. ONL represents outer nuclear layer; INL represents inner nuclear layer; GCL represents ganglion cell layer; NFL represents nerve fiber layer.

There are two structurally distinct types of outgrowth: the first occurs as loose arrays of short outgrowths (Figure 5, arrowhead; Figure 14) that terminate within the ONL. The other type appears as long processes with a variety of morphologies that cross the ONL either singly (examples are shown in Figure 7A-F, Figure 8A) or in larger arrays (Figure 5, arrow). To determine if the shorter processes terminate adjacent to withdrawn rod terminals we used α-VAMP2 (synaptobrevin) to label the photoreceptor terminals. In control cat retina labeled with α-VAMP2 (green channel), α-neurofilament (blue channel) and α-calretinin (red channel), the synaptic terminals (green) form a compact layer and no HC outgrowths project into the ONL (Figure 6A, asterisks). After detachment this highly organized layer loosens and disassembles. Some rod spherules retract as evidenced by numerous rod somata whose basal perinuclear cytoplasm labels with the VAMP2 antibody (arrowheads, Figure 6B). Figure 6B also shows a short HC outgrowth (arrow) projecting to a retracted, α-VAMP2-labeled rod terminal in the retina detached for 28 days. Based on many observations, the short outgrowths that end within the ONL usually terminate adjacent to these retracted terminals. Figure 7A (arrowheads) shows additional examples of the "directed" HC outgrowths in addition to the other type of outgrowth to the right (arrow). The latter can occur as a single, stout cylindrical or a ribbon-like process that extends across the ONL without branching, often to the subretinal space. Additional examples of this type of outgrowth (Figure 7B-F, Figure 8A, Figure 11 through Figure 13) display some of the variations in morphology that we have encountered. Some are smooth and of uniform caliber (Figure 7B, Figure 12, Figure 13); others are beaded (Figure 7C, Figure 11) or have a single varicosity (Figure 7E), while others appear swollen (Figure 7D, Figure 8A). All of them, however, arise from the outermost, red processes of the OPL. In fact, both types of outgrowth always are red, never displaying the bluish white or pink signature associated with the A-type HC. Although these outgrowths invariably stain most robustly with α-calretinin, they are also positive for α-calbindin D and even demonstrate some weak α-neurofilament labeling. This can be demonstrated by viewing images from the three channels separately (Figure 8A-D). Figure 8 shows one of the triple-labeled "undirected" processes ascending through the ONL. Figure 8A is the merged image from all three channels. Figure 8B shows the same process viewed through the α-calretinin

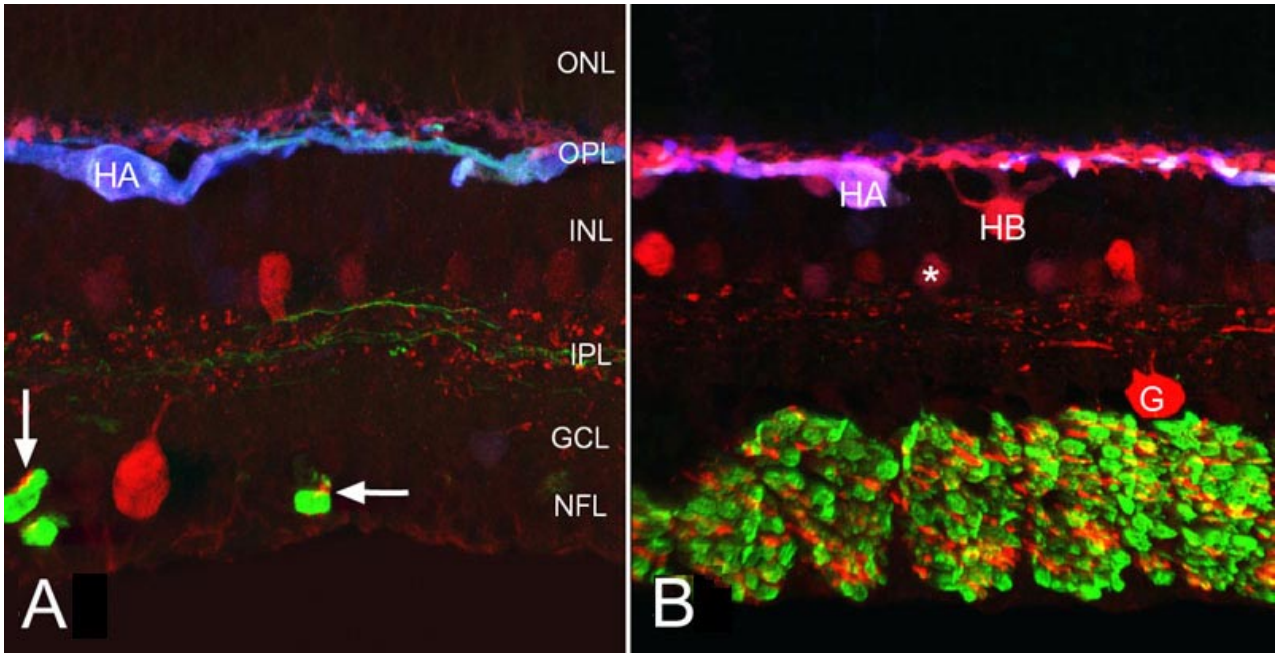

Figure 3. Confocal micrographs of triple labeled cat retina. Confocal micrographs of cat retina triple labeled with antibodies to calretinin (red), neurofilament (green) and calbindin D (blue). **A**: Normal cat retina. Two red, anti-calretinin-positive neurons lie on either side of the inner plexiform layer (IPL). An axonless HC (HA), labeled by all three probes, appears blue in this image, while the other HCs strongly labeled with anti-calretinin and less so with anti-calbindin D, remain reddish. Anti-neurofilament labeling is also evident in the nerve fiber layer (NFL) and processes running in the middle and outermost layers of the IPL. Note the anti-calretinin-positive fibers (arrows) in these fiber bundles. ONL represents outer nuclear layer; INL represents inner nuclear layer; GCL represents ganglion cell layer. **B**: Normal cat retina. Closer to the optic nerve head, the nerve fiber bundles are much larger than in **A**; a minority of these fibers lack neurofilament protein, but are anti-calretinin-positive. An anti-calretinin-positive ganglion cell (G) sends processes into the middle of the IPL. Two amacrine cells in the INL are brightly labeled with anti-calretinin; AII amacrine cells (*) stain less intensely with this antibody. The axonless HC (HA), labeled by all three probes, has a light violet hue; the cell body of the axon-bearing type (HB) and its dendrites remain red. The perikaryon of the B-type HC lies deeper in the INL than does the more planar HA type. **B** is reprinted from Progress in Retinal and Eye Research, 24, S. K. Fisher, G. P. Lewis, K. A. Linberg and M. R. Verardo, "Cellular remodeling in mammalian retina: results from studies of experimental retinal detachment," 395-431, 2006, with permission from Elsevier.

channel where the signal is strongest, while Figure 8C and Figure 8D, respectively show the significantly weaker signals from the α-neurofilament and α-calbindin D channels. This series also demonstrates the labeling patterns of an A-type HC with these same antibodies (white processes in Figure 8A). In Figure 8C the weak staining of the outgrowth with α-neurofilament antibody contrasts with its robust staining of the A-type HC and its processes that are known to contain many neurofilaments [1]. These HC outgrowths are common in the detached retinas, and all that we have observed appear to arise from processes that have the same relatively weak expression of neurofilament protein.

When these outgrowths reach the subretinal space, many appear to end without branching (Figure 7A-E, Figure 12, Figure 13) thus appearing as an isolated example of the processes that often appear as "sprays" which terminate before reaching the subretinal space (Figure 5, arrow); others dilate abruptly and then arborize into several thick branches that spread laterally on the retinal surface and elaborate still finer processes (Figure 7F, Figure 11). (Figure 11 through Figure 13 are derived from z-series files and are presented as movies in the online version of this publication). The extent to which these radial, α-calretinin-positive outgrowths arborize can best be appreciated in wholemounts viewed en face at the level of the subretinal surface (Figure 9A,B). The branched neurites appear planar but Figure 9A, for example, consists of over twenty, 1 μm thick optical sections. At lower magnification (Figure 9B) one can appreciate how dense the subretinal branching can be. We have previously demonstrated that these neurites ramify through and across the outer retinal surface in intimate association with hypertrophied Müller cell processes [5]. Figure 10A-F follow two individual thin processes beginning in the subretinal space (arrows, Figure 10A) down through the ONL (Figure 10B,C) to their connections at the outer edge of the OPL (Figure 10D-F). At this point the outgrowths join with a tangle of similarly stained processes making it hard to follow them very much further with any certainty. Nevertheless, we have examined many of these outgrowths serially both in wholemount and in radial aspect, and they always connect to a tangle of fine red, filigreed processes, never to thick dendritic trunks let alone to A-type bluish-white processes. We feel confident that these connections are made with the dense axon terminal plexus of the B-type cell.

Some of the most compelling evidence in support of this hypothesis is shown in Figure 14, a single image taken from a z series of 160, 0.5 μm thick optical sections through the outer

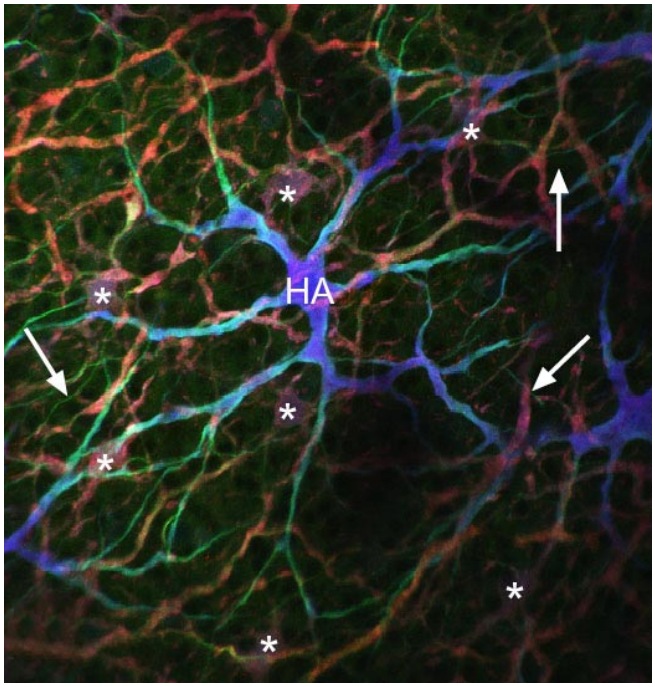

Figure 4. An axonless A type HC in a 7 day wholemounted retina. Wholemount of a 7 day detached retina labeled as in Figure 3. The triple-labeled axonless A type HC (HA) appears bluish-white. The greenish tinge to its distal-most dendrites suggests that more neurofilament protein is expressed there relative to the perikaryon and primary dendrites. Five reddish cell bodies of B-type HCs (*) lie deeper in the INL. Uniformly thin greenish processes (arrows) are likely the axons of the B-type cell showing an upregulation of neurofilament protein in response to retinal detachment. Reprinted from Progress in Retinal and Eye Research, 24, S. K. Fisher, G. P. Lewis, K. A. Linberg and M. R. Verardo, "Cellular remodeling in mammalian retina: results from studies of experimental retinal detachment," 395-431, 2006, with permission from Elsevier.

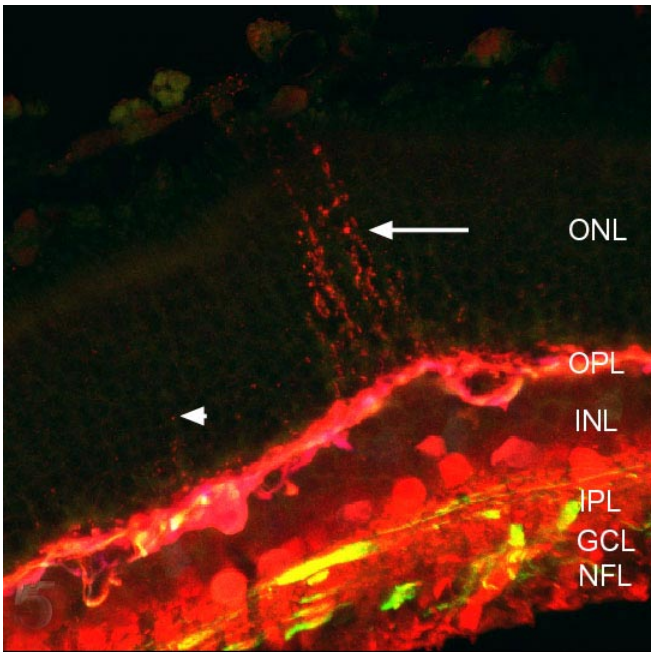

Figure 5. Triple labeled 7 day detached cat retina. A 7 day detached cat retina triple labeled with antibodies against calretinin (red), neurofilament (green) and calbindin D (blue). A large array of beaded HC outgrowths (arrow) rises more than halfway through the outer nuclear layer (ONL) while shorter arrays (arrowhead) also originate from the red, anti-calretinin-dominated processes of the distal outer plexiform layer (OPL). Anti-neurofilament-positive processes are more numerous in the inner plexiform layer (IPL) and ganglion cell layer (GCL). INL represents inner nuclear layer; NFL represents nerve fiber layer.

retina of a wholemount from a 28 day detached retina labeled by α-calretinin. When the wholemount was studied at various optical depths by 2-photon microscopy, we were fortunate enough to find two strongly labeled structures that are almost certainly B-type HC axon terminals (Figure 14, HBat1, HBat2). At the angle of rotation shown in Figure 14 (The rotation of the whole series is presented as a movie in the online version of this publication), these two structures appear to arise from two thin, parallel, strongly stained axons (ax1, ax2). Both their morphology and their degree of calretinin immunoreactivity clearly differentiate them from the A-type cell (HA) lying along the border of the OPL and INL. As the series is rotated to produce a view about 90°from the plane of the wholemount (i.e., when the retina is 'thinnest' and the retinal layers most clearly defined), fine 'sprays' of beaded processes arise from these presumed HBats and extend nearly across the ONL, most clearly resembling the processes shown in cross-section in Figure 5. Other processes orthogonal to these sprouts, presumably representing the original telodendria, appear in the plane of the OPL. It is striking that these HBats have less complex branching than might have been expected based on their known complexity (see Figure 1). This is probably due to the fact that both growth and pruning of these processes occur in response to the loss of rod terminals.

DISCUSSION

In the process of studying experimental retinal detachment using a feline model system, we have observed a surprising degree of rapid structural remodeling on the part of adult neurons [3,8]. Similar changes have been observed in a variety of inherited retinal degenerations, although in those cases the remodeling may occur over a longer period of time [25-33]. We first described robust neurite sprouting by rod bipolar cells and HCs occurring within 1 day of detachment [3], and later a similar response on the part of ganglion cells [8]. The original descriptions of HC outgrowths were from retinal sections labeled with an antibody to calbindin D that labels both types of cat HC [18]. After retinal detachment, two types of beaded, calbindin D-positive outgrowths were described invading the ONL: short processes that appear "directed" terminate adjacent to retracted rod terminals; and those that appear "undirected" in the sense that they grow across the ONL into the subretinal space. The latter occur singly or in large sprays comprised of multiple, parallel outgrowths that are seen most often after detachment periods of 7 to 28 days and usually in association with hypertrophic Müller cell outgrowths [5,8-10]. There are also a small number of outgrowths descending into the INL. We focused on the shorter processes directed towards retracted rod terminals and the long, undirected processes that

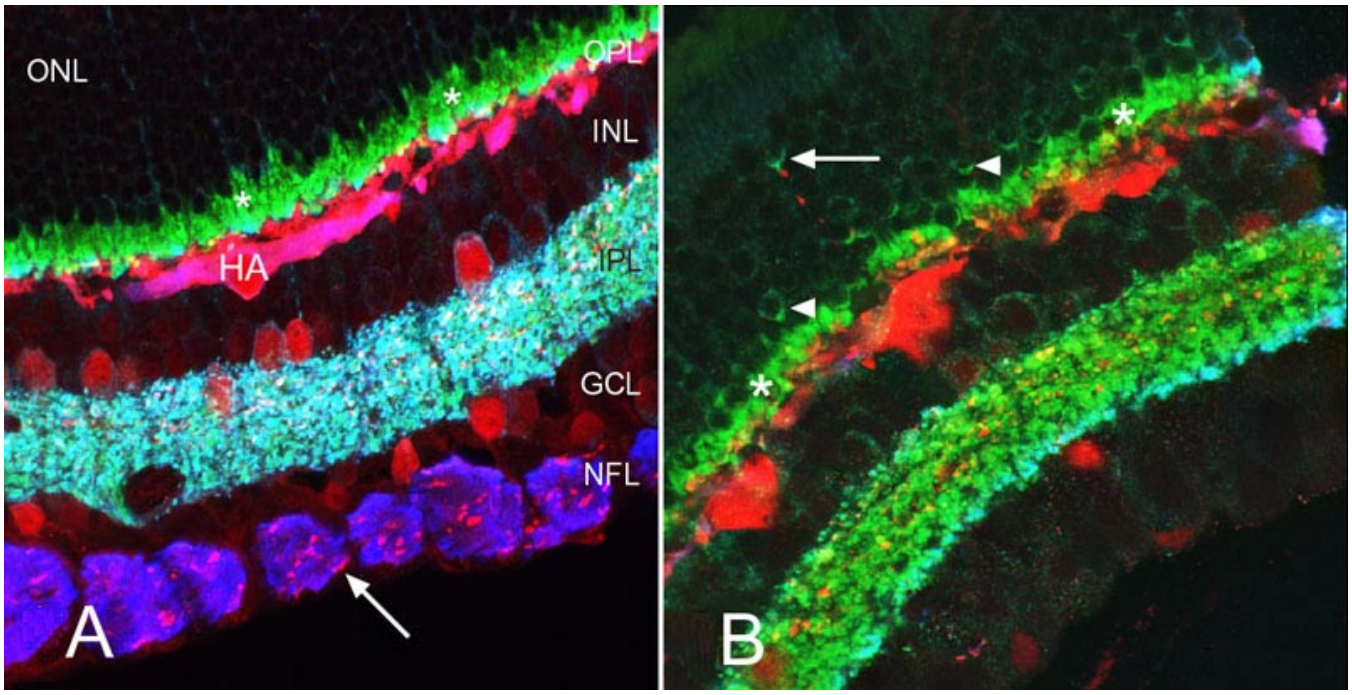

Figure 6. Confocal micrographs of triple labeled cat retina. Confocal images of retina triple labeled with antibodies against calretinin (red), neurofilament (blue) and VAMP2 (synaptobrevin, green). **A**: Normal cat retina. An A-type HC has pinkish primary dendrites that underlie the red processes of the distal outer plexiform layer (OPL). The antibody to the synaptic vesicle protein VAMP2 labels the terminals of both rods and cones forming a thick uninterrupted layer (*) overlying the labeled HC processes; it also labels synaptic terminals in the inner plexiform layer (IPL). No HC processes extend beyond the boundaries of the OPL. Anti-calretinin-positive fibers (arrow) lie among anti-neurofilament-positive fibers running in bundles in the nerve fiber layer (NFL) in this section from central retina. ONL represents outer nuclear layer; INL represents inner nuclear layer; GCL represents ganglion cell layer. **B**: 28 day detached cat retina. The layer of labeled cone and rod terminals has thinned and is discontinuous (*) as shown by the VAMP2 labeling. Basal, perinuclear labeling by VAMP2 (arrowheads) can be seen in a number of rod nuclei in the proximal ONL. A short HC outgrowth (arrow) appears directed to a retracted rod terminal labeled by the VAMP2 antibody.

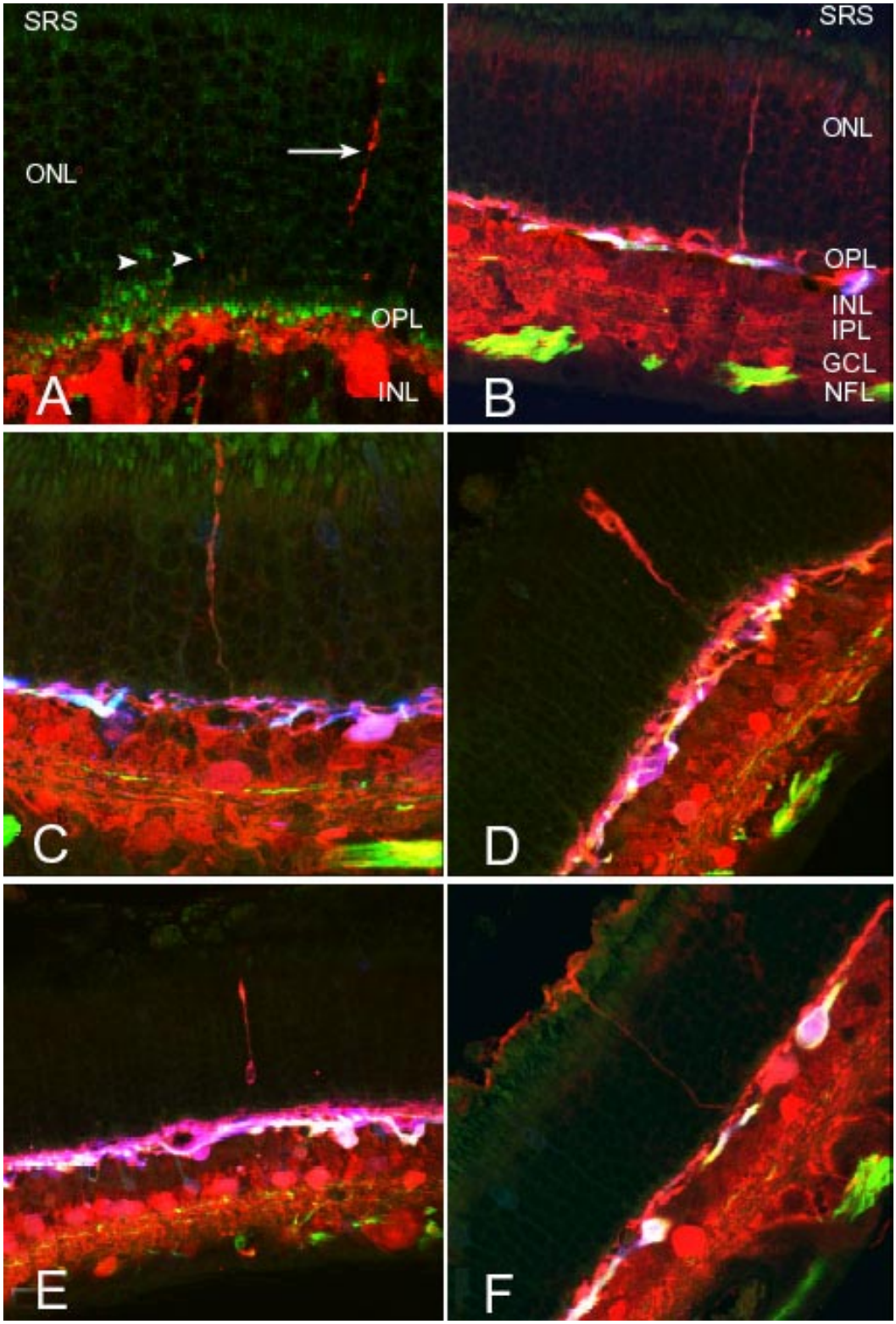

Figure 7. Confocal images of "undirected" HC outgrowths. Confocal images of isolated HC outgrowths most commonly seen in detachments of longer duration. **A**: Double labeled 7 day detached cat retina. A number of short beaded processes (arrowheads) label with the calretinin antibody (red) and appear directed to retracted rod terminals labeled with the antibody to VAMP2 (green). To the right, a long, unbranching outgrowth (arrow) crosses the outer nuclear layer (ONL) and appears undirected with respect to rod terminals. SRS represents subretinal space; OPL represents outer plexiform layer; IPL represents inner plexiform layer. **B**: Triple labeled 28 day detached cat retina labeled with antibodies against calretinin (red), neurofilament (green) and calbindin D (blue). A red, predominantly anti-calretinin-positive HC outgrowth rises from red processes in the distal outer plexiform layer (OPL) and crosses the outer nuclear layer (ONL). SRS represents subretinal space; INL represents inner nuclear layer; IPL = inner plexiform layer; GCL represents ganglion cell layer; NFL represents nerve fiber layer. **C**: 28 day detached retina labeled as in **B** above and in **D** to **F** below. Another red anti-calretinin-positive outgrowth rises through the ONL to the subretinal space. It is unbranched, but has multiple varicosities along its length. **D**: 7 day detached retina. A red anti-calretinin-positive HC outgrowth rising from the outer OPL appears to broaden as it crosses the ONL. **E**: 7 day detached retina. Yet another red anti-calretinin-positive HC outgrowth rises into the ONL and has a large varicosity in the inner ONL. **F**: 7 day detached cat retina. A reddish 'undirected' HC outgrowth rises from the outermost portion of the OPL and passes through the ONL without branching. The ascending fiber maintains a uniform caliber and lacks beads or varicosities. Once at the level of the subretinal space, it gives rise to processes spreading horizontally along the retinal surface. There are no outgrowths rising from the pinkish to white A-type cells. Indeed, in **B** through **F**, a plexus, of whitish A-type HC processes courses through the lower OPL without participation in any of these outgrowths. **B** and **F** reprinted from Progress in Retinal and Eye Research, 24, S. K. Fisher, G. P. Lewis, K. A. Linberg and M. R. Verardo, "Cellular remodeling in mammalian retina: results from studies of experimental retinal detachment," 395-431, 2006, with permission from Elsevier.

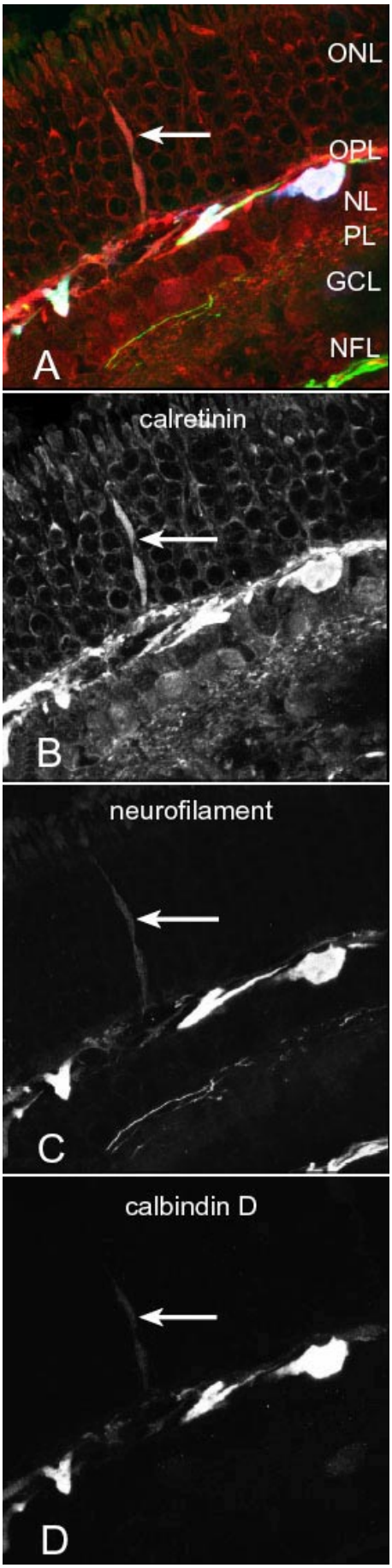

occur singly (rather than in the arrays) because we could more accurately follow their course in serial optical sections. All the outgrowths have the same antibody labeling characteristics.

Insofar as cats have two types of HC [1,2,11], a major question was whether one or both types gives rise to these neurites? One possible interpretation of our earlier data was that the directed processes originated from the B-type axon terminal (because they terminate adjacent to rod spherules) while the undirected processes arose from the dendrites of A- and/or B-type cells, perhaps representing more of an overall, more generalized response on the part of second order neurons to photoreceptor degeneration. Taken together we believe the current data supports the hypothesis that all of the outgrowths originate from the axon terminal system of the B-type cell. First, we were able to use the α-VAMP2 immunostaining to confirm earlier results suggesting that the fine neurites terminating in the ONL invariably end adjacent to withdrawn rod terminals, the normal target of the B-type axon terminal telodendria [12]. Secondly, both the directed and undirected processes have an immunocytochemical signature characteristic of the B-type cell. While it is interesting that these cells appear to slightly increase their neurofilament protein content after detachment, the level of staining with the antibody never reaches that of the A-type cell. Thirdly, when followed into the subretinal space, the single thin processes dilate suddenly before branching further as if attempting to form a rudimentary axon terminal in this new environment. Fourth, when a single process is traced back to the OPL it always appears to arise from a dense tangle of processes in the correct stratum and with the correct immunocytochemical signature to be the branching axon terminal. And fifth, in the large z series shown in Figure 14, there are clear examples of processes arising from axon terminals ending deep in the ONL.

Given that the neurites arising after detachments showed weak labeling with antibodies to the neurofilament protein, it seemed possible that the neurofilament-rich A-type cell [1] might be their source. However, the dendrites of this axonless HC contacts cones only [12] and cones do not show the same

Figure 8. A triple-labeled HC outgrowth seen in each channel. A series of confocal images of the same HC outgrowth from a retina detached for 28 days and triple labeled as described above in Figure 7B. **A**: A reddish triple-labeled outgrowth rises from processes of the same hue in the outermost outer plexiform layer (OPL). Examining each channel independently demonstrates that this outgrowth is labeled with all three antibody probes. ONL represents outer nuclear layer; INL represents inner nuclear layer; IPL represents inner plexiform layer; GCL represents ganglion cell layer; NFL represents nerve fiber layer. **B**: The outgrowth labels most intensely with the calretinin antibody that strongly labels both types of HC as well as several types of amacrine cell. **C**: Antibodies to neurofilament protein strongly label the A-type HC, but also weakly stain the B-type cell. This same weak labeling can be seen in the outgrowth (arrow). Most of the fibers in nerve fiber layer are strongly labeled as are certain ganglion cell processes in the mid-IPL. **D**: The antibody to calbindin D intensely labels the A-type HC [18], while the B-type, as well as the outgrowth (arrow), are weakly labeled.

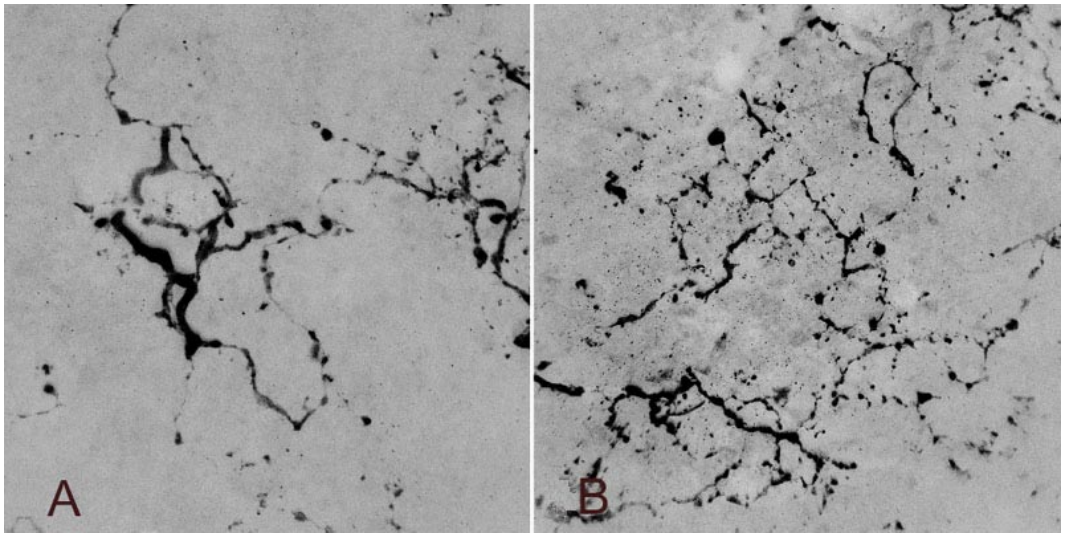

Figure 9. Two HC outgrowths at the retinal surface seen en face. Confocal images of retinal wholemounts of cat retina detached for 28 days taken at the outer retinal surface. The images have been digitally inverted and enhanced using Abode Photoshop. **A**: Seen en face, two anti-calretinin-positive HC outgrowths gives rise to multibranched and beaded arrays of processes that spread laterally over the retinal surface. While these arborizations appear planar, this "z-series" consists of 20 μm thick optical sections. **B**: At lower magnification, the multiple arborizations of six outgrowths crowd the retinal surface. Figure 9A is reprinted from Progress in Retinal and Eye Research, 24, S. K. Fisher, G. P. Lewis, K. A. Linberg and M. R. Verardo, "Cellular remodeling in mammalian retina: results from studies of experimental retinal detachment," 395-431, 2006, with permission from Elsevier.

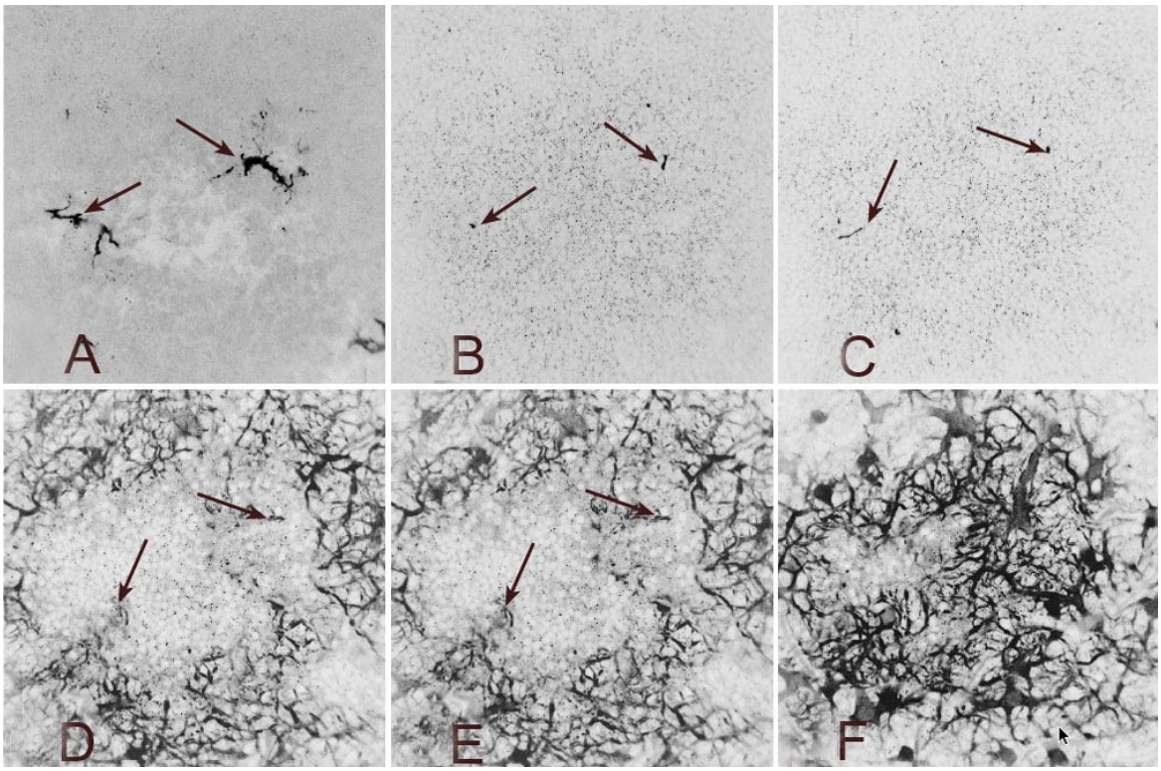

Figure 10. A sequence of confocal images of two HC outgrowths that span the ONL. Images selected from a serial z series through the outer retina. Two HC outgrowths from a wholemount of cat retina detached for 28 days and labeled with an antibody to calretinin. Image processing as in Figure 9. **A**: The arboreal trunks of the two outgrowths spread laterally at the exposed photoreceptor surface. **B**: Descending into the outer ONL, the two fibers (arrows) connecting to these outer arborizations can be seen. **C**: The same two outgrowths (arrows) still deeper in the ONL. One (to the left) runs obliquely in the plane of section. **D**: At the outermost portion of the OPL, these two fibers connect to their processes of origin (arrows). **E**: These fibers can be traced for a few sections further (arrows) before being lost in the red tangle of anti-calretinin-positive processes resident to the outer OPL, as seen in **F**.

reactive retraction of their terminals as rods [5,9]. Since one of the subsets of neurites appears to be specifically "directed" to retracted rod spherules, the initial trigger for the sprouting response logically could be the retraction of the rod terminals from the outer OPL. Such neurites would thus sprout from the HC domain that normally innervates the receding terminals. But what stimulates the other outgrowths that grow through the ONL and into the subretinal space? It might be that they arise secondarily, as a result of some general "activation" of the axon terminals since they are most frequently observed in detachments of longer duration. Or they may be neurites that do not encounter retracted rod spherules (i.e., one of the multiple processes forming the arrays as shown in Figure 5) and simply continue to grow across the ONL, perhaps being guided through their association with reactive Müller cell processes [5,9,10]. Why they would expand and branch in the subretinal space, almost appearing to recapitulate the axon terminal morphology, remains a mystery.

Although the presence of neurofilament protein in axon-bearing HCs has been reported by Peichl and González-Soriano [34] in mouse retina, this cytoskeletal protein has been assumed, based on ultrastructural evidence, to be absent or expressed at very low levels in normal, feline B-type HCs [1]. Although neurofilament protein does appear to be slightly up-regulated in the B-type cell after detachment, its parallel up-regulation in the A-type cell results in even more intense labeling than in control retina [9]. Indeed, this in itself is an interesting reaction on the part of these retinal neurons. An increase in the intermediate filament proteins GFAP and vimentin in glial cells after CNS injury is generally associated with extensive structural remodeling [35]. If that is also true for neurons, then the substantial up-regulation of intermediate filament proteins in the A-type cell may suggest structural changes in this cell type as well. Cones would be the likely

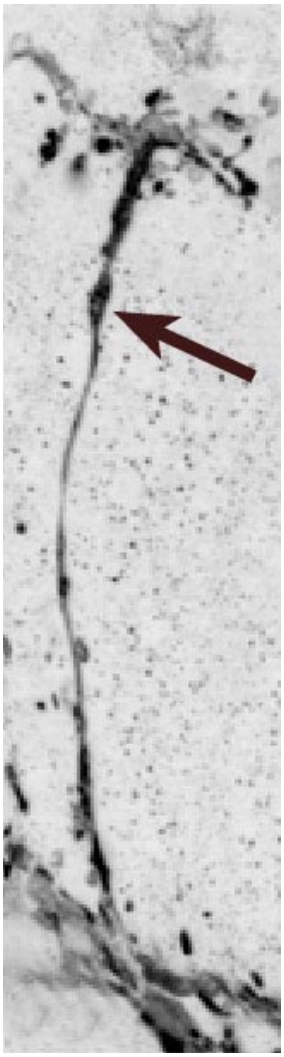

Figure 11. Confocal micrograph of an anti-calretinin-positive HC outgrowth in a section of cat retina that has been detached for 28 days. Confocal micrograph of an anti-calretinin-positive HC outgrowth in a section of cat retina that has been detached for 28 days. This process rises from the OPL and branches distally (arrow) near the retinal surface. This image is one in a series of 38 optical sections harvested at 0.3 μm intervals that are compiled as an AVI movie loop. Both the digital image inversion and the AVI file were created using Image Pro Plus software. There is a quicktime movie of this figure in the online version of this article. A representative frame is included here.

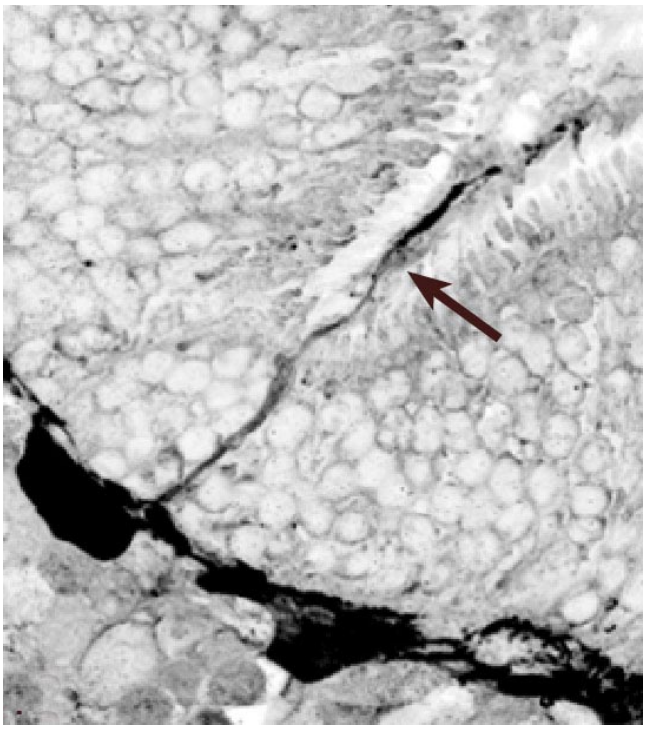

Figure 12. Confocal micrograph of a α-calretinin-positive HC outgrowth. Confocal micrograph of an α-calretinin-positive HC outgrowth (arrow) that extends across a narrowed ONL at a retinal fold in a 28 day detached cat retina. This is one in a series of 21 optical sections harvested at 0.3 μm intervals that are compiled as an AVI movie loop. Both the digitally inverted image and the AVI file were created using Image Pro Plus software. There is a quicktime movie of this figure in the online version of this article. A representative frame is included here.

partners in what may be subtle remodeling. Cone synaptic terminals do alter their morphology in response to detachment but generally remain "in place" in the OPL. Significantly, their deep synaptic invaginations [12,36,37] appear to be reduced or lost [9] which may induce subtle degrees of remodeling of the A- and B-cell dendrites. The fact that cone terminals do not retract would not require dramatic outgrowths of processes in order to maintain physical contact and thus, presumably, the capacity for molecular signaling. Since we have observed both the 'pruning' and outgrowth of dendrites from rod bipolar cells, similar reactions may occur among HC dendrites but may be difficult to detect. Although the lack of large numbers of branches on the two axon terminals shown in Figure 14 certainly suggests that pruning is a component of their responsiveness, planned experiments using the intracellular injection of fluorescent dyes and the examination of the cells in wholemounts should more readily reveal such subtle changes.

We know both rods and cones die after detachment [38,39], so it is also possible that the loss of presynaptic neurons triggers responses of the HCs. This may also be the case in the sprouting of HC neurites described as a consequence of long term retinal degenerations in RCS rats [25] and in humans afflicted with retinitis pigmentosa [26] or after retinal detachment [40]. Such a HC response is not universal however. While detachment results in the wholesale loss of virtually all photoreceptors in the cone-dominated ground squirrel retina [41], no neurite sprouting from second order neurons has been observed. But also in this species, Müller cells are almost unreactive, again reinforcing the idea of a functional interaction between the two.

Nothing we present here can give a definitive answer to the functional purpose of the extensive remodeling of these neurons. But, compared to ground squirrel retina where there appears to be little response to detachment by neurons, RPE cells or Müller cells [41], the cat's retina shows a vigorous, energy-requiring series of responses to such trauma. Certainly it is widely believed that severing synaptic connections between neurons can result in molecular and structural changes in both the innervating cell and target cell as well, sometimes even affecting the survival of one or both [42,43]. It is interesting that while HCs are interneurons that are small compared to sensory or motor neurons of the CNS, our data suggest that they still show a distinctive difference between the reactivity of their dendrites and axons. In these cells the thin axon serves mainly as a metabolic link between two electrically independent domains of the same cell [44]. If anything, the ability of the axon terminal system to sprout neurites (while the dendritic system seems relatively quiescent) underscores this independence even more and does suggest a functional intent to such structural plasticity.

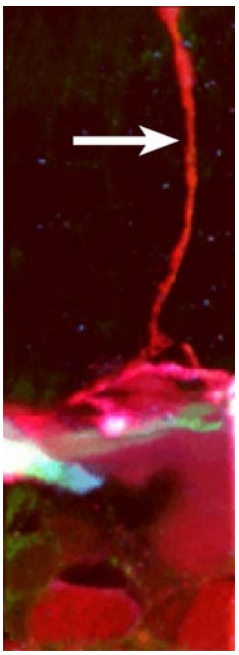

Figure 13. Confocal micrograph of an HC outgrowth from a plexus of processes in the distal OPL. The tissue was triple labeled with antibodies against calretinin (red channel), neurofilament (green channel) and calbindin D (blue channel). The outgrowth (arrow) and the OPL processes from which it arises are red in color whereas the processes and perikarya of A-type HCs are white to bluish in hue. This image is one in a series of 46 optical sections harvested at 0.3 μm intervals that are compiled as an AVI movie loop. Image Pro Plus software was used to digitally crop the image and to create the AVI file. There is a quicktime movie of this figure in the online version of this article. A representative frame is included here.

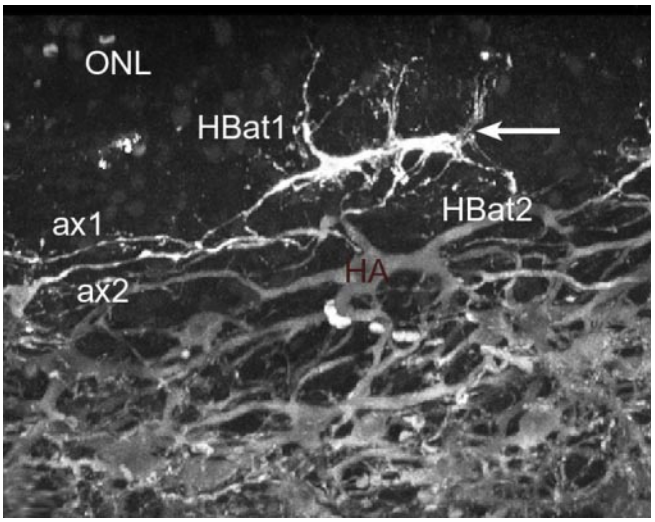

Figure 14. Wholemount of a 28 day detached retina labeled with the antibody to calretinin conjugated to donkey-a-rabbit AMCA. Wholemount of a 28 day detached retina, labeled with the antibody to calretinin conjugated to donkey-a-rabbit AMCA, that shows several 'directed' neurites rising into the outer nuclear layer (ONL) from a pair of B-type axon terminals (HBat1, HBat2) lying distal to an A-type perikaryon (HA) and its radiating dendritic trunks. The axons (ax1, ax2) and terminal processes of the B-type HCs stain more intensely than the A-type cell since the former has a greater affinity for the calretinin antibody than does the latter. This oblique projection was derived from a series of 160 0.5 mm thick optical sections captured by a Zeiss LSM 510 two-photon microscope and can be seen as a movie. There is a quicktime movie of this figure in the online version of this article. A representative frame is included here.

Conclusions: We have identified calretinin-positive outgrowths from HCs in the detached cat retina that appear to either associate with retracting rod terminals, or extend alongside reactive Müller cell extensions into the subretinal space. Our data suggest that they originate from the B-cell axon terminals. When these neurites reach the exposed photoreceptor surface, some give rise to fine, arborized structures that recapitulate, if crudely, axon terminal branching patterns. Thus the remodeling we have demonstrated appears to be a highly specific response of the axon terminal of the B-type cell.

Ultimately, the kinds of plasticity described here by mature neurons in response to serious retinal injury may have major implications for vision in humans where many of these same responses have been reported [40]. Many studies have brought to light a series of unique but conserved neural pathways through the retina that are responsible for various visual tasks [45,46]. We don't know if the directed outgrowths of rod bipolar dendrites and B-type axon terminals help preserve these pathways during an episode of photoreceptor deconstruction such as occurs after detachment, but it is a plausible hypothesis. They may also provide a mechanism for rapid recovery of the rod system upon reattachment by maintaining circuitry that otherwise would have to be formed de novo. It is more difficult to hypothesize a purpose for the undirected outgrowths. Perhaps they are simply the result of an overall response to injury on the part of the axon terminal. It could be that a "directed" outgrowth connected to a retracted rod terminal may transition to an "undirected" process if its presynaptic terminal degenerates or its target rod photoreceptor dies.

Although morphologically different from those in feline retina, human HCs are organized similarly with their dendrites connected to cones and their axon terminals to rods. The feline retina appears to reflect accurately other changes in human detachments such as outer segment degeneration, rod terminal retraction and neurite outgrowths from second and third order neurons [40] and is thus a reasonable model in which to study events relevant to the human retina's response to injury.

ACKNOWLEDGEMENTS

The authors wish to acknowledge the technical expertise of Ms. Katrina M. Carter and Mr. Kellen Betts. This study was supported by NIH grant EY00888 to S.K.F. and NSF grant ITR-0331697.

REFERENCES

1. Fisher SK, Boycott BB. Synaptic connections made by horizontal cells within the outer plexiform layer of the retina of the cat and the rabbit. Proc R Soc Lond B Biol Sci 1974; 186:317-31.
2. Boycott BB, Peichl L, Wässle H. Morphological types of horizontal cell in the retina of the domestic cat. Proc R Soc Lond B Biol Sci 1978; 203:229-45.
3. Lewis GP, Linberg KA, Fisher SK. Neurite outgrowth from bipolar and horizontal cells after experimental retinal detachment. Invest Ophthalmol Vis Sci 1998; 39:424-34.
4. Wässle H, Boycott BB, Peichl L. Receptor contacts of horizontal cells in the retina of the domestic cat. Proc R Soc Lond B Biol Sci 1978; 203:247-67.
5. Fisher SK, Lewis GP. Müller cell and neuronal remodeling in retinal detachment and reattachment and their potential consequences for visual recovery: a review and reconsideration of recent data. Vision Res 2003; 43:887-97.
6. Anderson DH, Stern WH, Fisher SK, Erickson PA, Borgula GA. Retinal detachment in the cat: the pigment epithelial-photoreceptor interface. Invest Ophthalmol Vis Sci 1983; 24:906-26.
7. Erickson PA, Fisher SK, Anderson DH, Stern WH, Borgula GA. Retinal detachment in the cat: the outer nuclear and outer plexiform layers. Invest Ophthalmol Vis Sci 1983; 24:927-42.
8. Coblentz FE, Radeke MJ, Lewis GP, Fisher SK. Evidence that ganglion cells react to retinal detachment. Exp Eye Res 2003; 76:333-42.
9. Fisher SK, Lewis GP, Linberg KA, Verardo MR. Cellular remodeling in mammalian retina: results from studies of experimental retinal detachment. Prog Retin Eye Res 2005; 24:395-431.
10. Lewis GP, Fisher SK. Retinal plasticity and interactive cellular remodeling in retinal detachment and reattachment. In: Pinaud R, Tremere LA, De Weerd P, editors. Plasticity in the visual system: from genes to circuits. New York: Springer; 2006. p. 55-78.
11. Dowling JE, Brown JE, Major D. Synapses of horizontal cells in rabbit and cat retinas. Science 1966; 153:1639-41.
12. Kolb H. The connections between horizontal cells and photoreceptors in the retina of the cat: electron microscopy of Golgi preparations. J Comp Neurol 1974; 155:1-14.
13. Wässle H, Peichl L, Boycott BB. Topography of horizontal cells in the retina of the domestic cat. Proc R Soc Lond B Biol Sci 1978; 203:269-91.
14. Linberg KA, Lewis GP, Carter KM, Fisher SK. Immunocytochemical evidence that B-type horizontal cell axon terminals remodel in response to experimental retinal detachment in the cat. ARVO Annual Meeting; 2004 April 25-29; Fort Lauderdale (FL).
15. Lewis GP, Linberg KA, Geller SF, Guérin CJ, Fisher SK. Effects of the neurotrophin brain-derived neurotrophic factor in an experimental model of retinal detachment. Invest Ophthalmol Vis Sci 1999; 40:1530-44.
16. Hale IL, Matsumoto B. Resolution of subcellular detail in thick tissue sections: immunohistochemical preparation and fluorescence confocal microscopy. In: Matsumoto B, editor. Cell biological applications of confocal microscopy. 2nd ed. San Diego: Academic Press; 2002. p. 301-35.
17. Linberg KA, Lewis GP, Shaaw C, Rex TS, Fisher SK. Distribution of S- and M-cones in normal and experimentally detached cat retina. J Comp Neurol 2001; 430:343-56.
18. Pasteels B, Rogers J, Blachier F, Pochet R. Calbindin and calretinin localization in retina from different species. Vis Neurosci 1990; 5:1-16.
19. Goebel DJ, Pourcho RG. Calretinin in the cat retina: colocalizations with other calcium-binding proteins, GABA and glycine. Vis Neurosci 1997; 14:311-22.
20. Jeon MH, Jeon CJ. Immunocytochemical localization of calretinin containing neurons in retina from rabbit, cat, and dog. Neurosci Res 1998; 32:75-84.
21. Massey SC, Mills SL. Antibody to calretinin stains AII amacrine cells in the rabbit retina: double-label and confocal analyses. J Comp Neurol 1999; 411:3-18.
22. Mills SL, Massey SC. AII amacrine cells limit scotopic acuity in central macaque retina: A confocal analysis of calretinin labeling. J Comp Neurol 1999; 411:19-34.
23. Wässle H, Grünert U, Chun MH, Boycott BB. The rod pathway of the macaque monkey retina: identification of AII-amacrine cells with antibodies against calretinin. J Comp Neurol 1995;

361:537-51.
24. Kolb H, Zhang L, Dekorver L, Cuenca N. A new look at calretinin-immunoreactive amacrine cell types in the monkey retina. J Comp Neurol 2002; 453:168-84.
25. Chu Y, Humphrey MF, Constable IJ. Horizontal cells of the normal and dystrophic rat retina: a wholemount study using immunolabelling for the 28-kDa calcium-binding protein. Exp Eye Res 1993; 57:141-8.
26. Fariss RN, Li ZY, Milam AH. Abnormalities in rod photoreceptors, amacrine cells, and horizontal cells in human retinas with retinitis pigmentosa. Am J Ophthalmol 2000; 129:215-23.
27. Strettoi E, Pignatelli V. Modifications of retinal neurons in a mouse model of retinitis pigmentosa. Proc Natl Acad Sci U S A 2000; 97:11020-5.
28. Strettoi E, Porciatti V, Falsini B, Pignatelli V, Rossi C. Morphological and functional abnormalities in the inner retina of the rd/rd mouse. J Neurosci 2002; 22:5492-504.
29. Marc RE, Jones BW, Watt CB, Strettoi E. Neural remodeling in retinal degeneration. Prog Retin Eye Res 2003; 22:607-55.
30. Jones BW, Watt CB, Frederick JM, Baehr W, Chen CK, Levine EM, Milam AH, Lavail MM, Marc RE. Retinal remodeling triggered by photoreceptor degenerations. J Comp Neurol 2003; 464:1-16.
31. Pignatelli V, Cepko CL, Strettoi E. Inner retinal abnormalities in a mouse model of Leber's congenital amaurosis. J Comp Neurol 2004; 469:351-9.
32. Claes E, Seeliger M, Michalakis S, Biel M, Humphries P, Haverkamp S. Morphological characterization of the retina of the CNGA3(-/-)Rho(-/-) mutant mouse lacking functional cones and rods. Invest Ophthalmol Vis Sci 2004; 45:2039-48.
33. Mansergh F, Orton NC, Vessey JP, Lalonde MR, Stell WK, Tremblay F, Barnes S, Rancourt DE, Bech-Hansen NT. Mutation of the calcium channel gene Cacna1f disrupts calcium signaling, synaptic transmission and cellular organization in mouse retina. Hum Mol Genet 2005; 14:3035-46.
34. Peichl L, González-Soriano J. Unexpected presence of neurofilaments in axon-bearing horizontal cells of the mammalian retina. J Neurosci 1993; 13:4091-100.
35. Wilhelmsson U, Li L, Pekna M, Berthold CH, Blom S, Eliasson C, Renner O, Bushong E, Ellisman M, Morgan TE, Pekny M. Absence of glial fibrillary acidic protein and vimentin prevents hypertrophy of astrocytic processes and improves post-traumatic regeneration. J Neurosci 2004; 24:5016-21.
36. Boycott BB, Kolb H. The connexions between bipolar cells and photoreceptors in the retina of the domestic cat. J Comp Neurol 1973; 148:91-114.
37. Kolb H. The organization of the outer plexiform layer in the retina of the cat: electron microscopic observations. J Neurocytol 1977; 6:131-53.
38. Rex TS, Fariss RN, Lewis GP, Linberg KA, Sokal I, Fisher SK. A survey of molecular expression by photoreceptors after experimental retinal detachment. Invest Ophthalmol Vis Sci 2002; 43:1234-47.
39. Linberg KA, Lewis GP, Barawid EL, Sakai T, Fisher SK. A quantitative study of cone matrix sheath and S-cone recovery in reattached retina. ARVO Annual Meeting; 2002 May 5-10; Fort Lauderdale (FL).
40. Sethi CS, Lewis GP, Fisher SK, Leitner WP, Mann DL, Luthert PJ, Charteris DG. Glial remodeling and neural plasticity in human retinal detachment with proliferative vitreoretinopathy. Invest Ophthalmol Vis Sci 2005; 46:329-42.
41. Linberg KA, Sakai T, Lewis GP, Fisher SK. Experimental retinal detachment in the cone-dominant ground squirrel retina: morphology and basic immunocytochemistry. Vis Neurosci 2002; 19:603-19.
42. Kandell ER, Schwartz JH, Jessell TM, editors. Principles of neuroscience. 4th ed. New York: McGraw-Hill; 2000.
43. Gillingwater TH, Ribchester RR. Compartmental neurodegeneration and synaptic plasticity in the Wld(s) mutant mouse. J Physiol 2001; 534:627-39.
44. Nelson R, von Lützow A, Kolb H, Gouras P. Horizontal cells in cat retina with independent dendritic systems. Science 1975; 189:137-9.
45. Kolb H, Nelson R, Ahnelt P, Cuenca N. Cellular organization of the vertebrate retina. In: Kolb H, Ripps H, Wu SM, editors. Concepts and challenges in retinal biology: a tribute to John E. Dowling. 1st ed. Amsterdam: Elsevier. Prog Brain Res 2001; 131: 3-26.
46. Linberg K, Cuenca N, Ahnelt P, Fisher S, Kolb H. Comparative anatomy of major retinal pathways in the eyes of nocturnal and diurnal mammals. In: Kolb H, Ripps H, Wu SM, editors. Concepts and challenges in retinal biology: a tribute to John E. Dowling. 1st ed. Amsterdam: Elsevier. Prog Brain Res 2001; 131: 27-52.

The print version of this article was created on 29 Dec 2006. This reflects all typographical corrections and errata to the article through that date. Details of any changes may be found in the online version of the article.